

Large- Z atoms in the strong-interaction limit of DFT: Implications for gradient expansions and for the Lieb-Oxford bound

Timothy J. Daas,¹ Derk P. Kooi,¹ Tarik Benyahia,¹ Michael Seidl,¹ and Paola Gori-Giorgi¹

Department of Chemistry and Pharmaceutical Sciences, Amsterdam Institute of Molecular and Life Sciences (AIMMS), Faculty of Science, Vrije Universiteit, De Boelelaan 1083, 1081HV Amsterdam, The Netherlands

We study numerically the strong-interaction limit of the exchange-correlation functional for neutral atoms and for Bohr atoms as the number of electrons increases. Using a compact representation, we analyse an effective second-order gradient expansion, comparing it with the one for exchange (weak interaction limit). The two gradient expansions, at strong and weak interaction, turn out to be very similar in magnitude, but with opposite signs. We find that the point-charge plus continuum model is surprisingly accurate for the effective gradient expansion at strong coupling, while the PBE functional severely underestimates it. We then use our results to analyse the Lieb-Oxford bound from the point of view of slowly-varying densities, clarifying some aspects on the bound at fixed number of electrons.

I. INTRODUCTION

Exact properties (or constraints) of the exchange-correlation (XC) functional of Kohn-Sham (KS) density functional theory (DFT) play a central role in the construction of practical approximations (see, e.g., refs. 1–8). In particular, the slowly-varying limit,^{9–12} already invoked in the seminal paper of Kohn and Sham,¹³ has proven crucial for the development of generalised gradient approximations (GGA's), which was a key leap forward in making KS DFT the workhorse for computational chemistry and solid-state physics.⁸

While successful GGA's for solids⁶ typically recover the exact^{9–12} second-order gradient expansion coefficient for exchange, chemical systems are better described with GGA's with a coefficient almost twice as large in magnitude.^{1,14} This empirical observation was later rationalised by connecting the gradient expansion with the large- Z limit of neutral atoms, where Z is the nuclear charge.^{5,15} The argument partially relied on an assumption on the large- Z dependence of exchange beyond the local density approximation (LDA), which was recently corrected.^{16,17}

The exchange functional is the weakly-interacting (or high-density) limit of the exact XC functional. The opposite limit, strongly interacting (SIL) or low density,^{18–20} provides complementary information, and can be used to build approximations in different ways (for a recent review see ref. 20). The main aim of this work is to study the SIL functional for large- Z atoms, computing accurate numerical results and providing an analysis similar to the one done for exchange.^{15,17} To fully take into account the recent corrections on the large- Z limit for exchange,^{16,17} we analyse our results through the compact representation introduced in previous work on the strong-coupling limit of the Möller-Plesset adiabatic connection.¹⁶ We also perform this kind of compact analysis on exchange, which reveals a somewhat surprising symmetry between the two limits: the resulting effective gradient expansions are very similar in magnitude, but with opposite signs. As we shall see, our numerical study on neutral atoms and Bohr atoms also suggests a weak dependence on density profiles of this gradient expansion of both limits. We also compare our accurate results with different approximations.

We then turn to another important exact constraint for the XC functional: the Lieb-Oxford (LO) inequality.^{21–24} In previous

works,^{25–27} the SIL functional has been used to establish lower bounds for the optimal constant appearing in the LO inequality at given electrons number N .^{25–27} An open question that remained open in this context was why some densities give much better bounds than others. We will answer to this question by using the present results, and we will also investigate the relation with the functional appearing in the strong-coupling limit of the Möller-Plesset adiabatic connection.^{16,28,29} Hartree atomic units are used throughout.

II. THEORETICAL BACKGROUND

For a given N -electron density $\rho(\mathbf{r})$, the Levy³⁰-Lieb³¹ universal functional for general interaction strength λ is defined as

$$F_\lambda[\rho] = \min_{\Psi \rightarrow \rho} \langle \Psi | \hat{T} + \lambda \hat{V}_{ee} | \Psi \rangle, \quad (1)$$

where \hat{T} is the kinetic energy operator for the N electrons, \hat{V}_{ee} is their mutual Coulomb repulsion, and the minimization is performed over all many-electron wavefunctions with the prescribed density $\rho(\mathbf{r})$. The XC functional that needs to be approximated in any practical KS DFT calculation is

$$E_{xc}[\rho] = F_1[\rho] - F_0[\rho] - U[\rho], \quad (2)$$

where $U[\rho]$ is the Hartree (mean field) functional,

$$U[\rho] = \frac{1}{2} \int d\mathbf{r} \int d\mathbf{r}' \frac{\rho(\mathbf{r})\rho(\mathbf{r}')}{|\mathbf{r} - \mathbf{r}'|}. \quad (3)$$

A. The functionals $E_x[\rho]$ and $W_\infty[\rho]$

For the exact XC functional, applying uniform coordinate scaling by defining $\rho_\gamma(\mathbf{r}) = \gamma^3 \rho(\gamma\mathbf{r})$,

$$\int d\mathbf{r} \rho_\gamma(\mathbf{r}) = N \quad (\text{for all } \gamma > 0), \quad (4)$$

is equivalent^{32,33} to scale the strength of the electron-electron interaction, $\lambda = 1/\gamma$. The high ($\lambda \rightarrow 0$) and low ($\lambda \rightarrow \infty$) density limits (weakly and strongly interacting limits, respectively)

of the functional $E_{xc}[\rho]$ are known to be

$$\begin{aligned} \lim_{\lambda \rightarrow 0} (\lambda E_{xc}[\rho_{1/\lambda}]) &= W_0[\rho] \equiv E_x[\rho], \\ \lim_{\lambda \rightarrow \infty} (\lambda E_{xc}[\rho_{1/\lambda}]) &= W_\infty[\rho]. \end{aligned} \quad (5)$$

The high density ($\frac{1}{\lambda} \rightarrow \infty$) limit $W_0[\rho] = E_x[\rho]$ is also called the DFT exchange energy. Notice that both functionals satisfy

$$E_x[\rho_\gamma] = \gamma E_x[\rho], \quad W_\infty[\rho_\gamma] = \gamma W_\infty[\rho]. \quad (6)$$

If we look at the spin-polarization dependence, considering the spin-densities $\rho_\uparrow(\mathbf{r})$ and $\rho_\downarrow(\mathbf{r})$, with $\rho = \rho_\uparrow + \rho_\downarrow$, we have^{34–36}

$$E_x[\rho_\uparrow, \rho_\downarrow] = \frac{1}{2} E_x[\rho_\uparrow, \rho_\uparrow] + \frac{1}{2} E_x[\rho_\downarrow, \rho_\downarrow], \quad (7)$$

$$W_\infty[\rho_\uparrow, \rho_\downarrow] = W_\infty[\rho]. \quad (8)$$

The spin-independence of the functional $W_\infty[\rho]$ is due to the fact that, as $\lambda \rightarrow \infty$, electrons are strictly correlated, forming a floating crystal in a metric dictated by the density $\rho(\mathbf{r})$, with spin effects appearing at orders $\sim e^{-\sqrt{\lambda}}$.^{18,19,37} In the rest of this paper, we will consider closed-shell systems only, with $\rho_\uparrow = \rho_\downarrow = \rho/2$. Results for both functionals can be easily extended to open-shell systems via Eqs.(7)-(8).

B. Gradient expansion of $E_x[\rho]$ and $W_\infty[\rho]$

Central to many approximate XC functionals is the slowly varying limit, in terms of gradients of the density. The scaling relations of Eq. (6) imply that if a gradient expansion approximation (GEA) for the two functionals $W_i[\rho]$ ($i = 0$ or ∞) of Eq. (5) exists, its first two leading terms must be expressed using the integrals

$$I_0[\rho] = \int d\mathbf{r} \rho(\mathbf{r})^{4/3}, \quad (9)$$

$$I_2[\rho] = \int d\mathbf{r} \frac{|\nabla\rho(\mathbf{r})|^2}{\rho(\mathbf{r})^{4/3}}, \quad (10)$$

and must have the form

$$\begin{aligned} W_i[\rho] &= \underbrace{A_i \cdot I_0[\rho] + B_i \cdot I_2[\rho]}_{W_i^{\text{GEA2}}[\rho]} + \dots, \\ &= A_i \int d\mathbf{r} \rho(\mathbf{r})^{4/3} \left(1 + \frac{B_i}{A_i} \cdot x([\rho], \mathbf{r})^2 \right) + \dots \end{aligned} \quad (11)$$

In the second line, we have introduced the reduced gradient

$$x([\rho], \mathbf{r}) = \frac{|\nabla\rho(\mathbf{r})|}{\rho(\mathbf{r})^{4/3}}, \quad (12)$$

which essentially gives the relative change of the density on the scale of the average interparticle distance. In the DFT literature the equivalent reduced gradient $s([\rho], \mathbf{r}) = \frac{1}{2}(3\pi^2)^{-1/3} x([\rho], \mathbf{r})$ is often used, as it describes more accurately the relevant length scale in the uniform electron gas.

The LDA constants A_i are exactly known, while the value of the coefficients B_i is more subtle. By applying a slowly varying perturbation to the uniform electron gas, and by carefully handling the long-range Coulomb tail, a coefficient B_x^{GEA} for the exchange functional has been derived^{9–12} (we use equivalently $i = 0$ or $i = x$ to denote quantities for the functional $W_0 = E_x$). However, while GGA's that recover B_x^{GEA} work well for extended systems, for atoms and molecules better results are obtained with a value of magnitude roughly twice as large. In Table I we report a small overview, with some values of B_x for GGA exchange functionals widely used in chemistry.

For $W_\infty[\rho]$, the value of B_∞ is unknown. The point-charge plus continuum (PC) model,³⁵ provides an approximate value for this coefficient, as well as an approximate value for A_∞ , which is slightly different than the exact one. The PC model is constructed from the physical idea that for slowly varying densities the electrons will try to neutralise the small dipole created by the density gradient. The PC values are also reported in Table I, together with the B_∞ from the Perdew-Burke-Ernzerhof (PBE)¹ XC functional.

Gaining more information on the coefficient B_∞ is one of the aim of this article. To this purpose, in the following section III we will review particle number scaling⁵ and the large- Z limit of atoms^{5,17} as an alternative way to approach the slowly-varying limit for finite systems. Notice that this procedure is different than perturbing the uniform electron gas. While both procedures are expected to yield the same coefficients A_i ,³⁸ studies on the exchange functional^{5,17} found that the coefficient B_i is not the same, which could explain^{5,15,17} why successful GGA's for chemistry have $B_x \neq B_x^{\text{GEA}}$, as exemplified in Table I.

III. GRADIENT EXPANSION FROM PARTICLE-NUMBER SCALING

To investigate the gradient expansions in Eq. (11), we must consider densities ρ with weak (maximum) reduced gradient,

$$\max_{\mathbf{r} \in \mathbb{R}^3} x([\rho], \mathbf{r}) \ll 1, \quad (13)$$

and observe how the limit $x \rightarrow 0$ is approached. While perturbing a uniform density is one way to do that, adding more and more particles in a fixed density profile is another possibility, as detailed below.

A. Particle-number scaling of a density profile

For a given density profile $\bar{\rho}(\mathbf{r})$, with $\int d\mathbf{r} \bar{\rho}(\mathbf{r}) = 1$, (and for a given exponent p) we construct ("particle-number scaling") a sequence of densities,

$$\bar{\rho}_{N,p}(\mathbf{r}) = N^{3p+1} \bar{\rho}(N^p \mathbf{r}), \quad (14)$$

with increasing particle number N ,

$$\int d^3r \bar{\rho}_{N,p}(\mathbf{r}) = N \quad (N = 1, 2, 3, \dots). \quad (15)$$

$W_i[\rho]$	A_i	B_i
$E_x[\rho]$	$A_x = -\frac{3}{4}(\frac{3}{\pi})^{1/3} \approx -0.73856$	$B_x^{\text{GEA}} = -\frac{5}{216\pi(3\pi^2)^{1/3}} \approx -0.0024$ $B_x^{\text{B88}} = -0.0053$ $B_x^{\text{PBE}} = -0.0042$
$W_\infty[\rho]$	$A_\infty = -1.44423075$ $A_\infty^{\text{PC}} = -\frac{9}{10}(\frac{4\pi}{3})^{1/3} \approx -1.4508$	$B_\infty^{\text{GEA}} = ?$ $B_\infty^{\text{PC}} = \frac{3}{350}(\frac{3}{4\pi})^{1/3} \approx 0.0053173$ $B_\infty^{\text{PBE}} = 1.24457 \cdot 10^{-7}$

TABLE I. Coefficients A_i and B_i appearing in Eq. (11). The value of A_∞ is given by the bcc Wigner crystal energy, which is floating to recover the uniform density.³⁹ Values for the point-charge plus continuum (PC) model³⁵ and for the PBE¹ and B88¹⁴ functionals are also shown.

These densities have the reduced gradient

$$x([\bar{\rho}_{N,p}], \mathbf{r}) = \frac{x([\bar{\rho}], N^p \mathbf{r})}{N^{1/3}}. \quad (16)$$

Consequently, for sufficiently large particle numbers $N \gg 1$, they satisfy condition (13), provided that

$$\max_{\mathbf{r} \in \mathbb{R}^3} x([\bar{\rho}], \mathbf{r}) \quad \text{is finite.} \quad (17)$$

Using the densities (14) in Eq. (11), we see that the existence of a gradient expansion for the functionals $E_x[\rho]$ and $W_\infty[\rho]$ implies a well defined large- N expansion

$$\begin{aligned} W_i[\bar{\rho}_{N,p}] &= A_i \cdot I_0[\bar{\rho}_{N,p}] + B_i \cdot I_2[\bar{\rho}_{N,p}] + \dots \\ &= A_i \cdot I_0[\bar{\rho}] \cdot N^{p+4/3} + B_i \cdot I_2[\bar{\rho}] \cdot N^{p+2/3} + \dots \end{aligned} \quad (18)$$

Provided that the terms indicated by dots are sufficiently small, we may conclude

$$\begin{aligned} \frac{W_i[\bar{\rho}_{N,p}] - A_i \cdot I_0[\bar{\rho}] \cdot N^{p+4/3}}{I_2[\bar{\rho}] \cdot N^{p+2/3}} &= B_i + O(N^{-1/3}), \\ \lim_{N \rightarrow \infty} \frac{W_i[\bar{\rho}_{N,p}] - A_i \cdot I_0[\bar{\rho}] \cdot N^{p+4/3}}{I_2[\bar{\rho}] \cdot N^{p+2/3}} &= B_i. \end{aligned} \quad (19)$$

Notice that the uniform-coordinate scaling of Eq. (6) implies that all choices of p are equivalent for studying $E_x[\rho]$ and $W_\infty[\rho]$, since

$$W_i[\bar{\rho}_{N,p}] = N^p W_i[\bar{\rho}_{N,0}]. \quad (20)$$

For functionals that do not satisfy a simple relation under uniform coordinate scaling, such as the correlation functional, different values of p allow to explore different physical regimes, as reviewed in Ref. 40.

B. Densities with asymptotic particle-number scaling

Physical many-electron systems do not arise by filling more and more particles in a fixed density profile, but by adding particles in an external potential. In order to study the gradient expansion for physically relevant systems, several authors considered neutral atoms,^{5,15,17,41} in which $N = Z$ electrons are bound by a point charge Z , and so-called Bohr atoms,^{17,42,43} in which the external potential is $-1/r$ and the electron-electron interaction is set to zero. These systems define a sequence of N -electron densities $\rho_N^{\text{Sqc}}(\mathbf{r})$,

$$\int d\mathbf{r} \rho_N^{\text{Sqc}}(\mathbf{r}) = N \quad (N = 1, 2, 3, \dots), \quad (21)$$

which displays particle-scaling behavior only asymptotically (in the limit of large $N \gg 1$),

$$\rho_N^{\text{Sqc}}(\mathbf{r}) \approx \bar{\rho}_{N,p}^{\text{Sqc}}(\mathbf{r}) \quad (N \gg 1) \quad (22)$$

$$= N^{3p+1} \bar{\rho}^{\text{Sqc}}(N^p \mathbf{r}), \quad (23)$$

where $\bar{\rho}^{\text{Sqc}}(\mathbf{r})$ is an asymptotic density profile, specific for the sequence $\rho_N^{\text{Sqc}}(\mathbf{r})$, which can be obtained exactly from Thomas-Fermi (TF) theory.^{17,41-44}

In this case, using the densities $\rho_N^{\text{Sqc}}(\mathbf{r})$ in Eq. (11), we obtain, for large N ,

$$W_i[\rho_N^{\text{Sqc}}] = A_i \cdot I_0[\rho_N^{\text{Sqc}}] + B_i \cdot I_2[\rho_N^{\text{Sqc}}] + \dots \quad (24)$$

Unlike in Eq. (18), however, the N -dependence cannot be extracted explicitly here. Moreover, even when the integrals $I_{0,2}[\rho_N^{\text{Sqc}}]$ are finite for all values of N , the corresponding integrals $I_{0,2}[\bar{\rho}^{\text{Sqc}}]$ for the asymptotic profile $\bar{\rho}^{\text{Sqc}}(\mathbf{r})$ can be divergent, as we shall see below.

1. Neutral Atoms

We consider here the densities of neutral atoms (writing "na" for "Sqc"), $\rho_N^{\text{Sqc}}(\mathbf{r}) = \rho_N^{\text{na}}(\mathbf{r})$. In this case, we have asymptotically, as N gets larger and larger,^{41,44,45}

$$\begin{aligned} \rho_N^{\text{na}}(\mathbf{r}) &\approx \bar{\rho}_{N,1/3}^{\text{TFna}}(\mathbf{r}) \\ &= N^2 \bar{\rho}^{\text{TFna}}(N^{1/3} \mathbf{r}) \quad (p = \frac{1}{3}). \end{aligned} \quad (25)$$

The Thomas-Fermi profile $\bar{\rho}^{\text{TFna}}(\mathbf{r})$ does not have a closed form, but a very accurate parametrization is provided in Ref. 45. While $I_0[\bar{\rho}^{\text{TFna}}]$ has a finite value, $I_2[\bar{\rho}^{\text{TFna}}]$ diverges. This latter divergence has consequences for the large N (or, equivalently, large- Z) behavior of $E_x[\rho_N^{\text{na}}]$, which was somehow overlooked in earlier works^{5,6,15}, and was recently reconsidered.^{16,17} In particular, we have the large- N asymptotics

$$I_0[\rho_N^{\text{na}}] = a_1^{\text{na}} N^{5/3} + a_2^{\text{na}} N \log(N) + \dots \quad (26)$$

$$I_2[\rho_N^{\text{na}}] = b_1^{\text{na}} N \log(N) + b_2^{\text{na}} N + \dots, \quad (27)$$

where the values of the coefficients in the expansion are studied in Ref. 17.

In other words, condition (17) is not asymptotically satisfied for the sequence of neutral atom densities: there is a region (around the nucleus) in which the integrand in I_2 gets larger as N gets larger, although this region also effectively shrinks

with increasing N .^{17,41} Whether this is ultimately the reason for the value of B_x larger (in magnitude) than B_x^{GEA} in successful GGA's for chemical systems seems to remain an open question.¹⁷

2. Bohr atoms

The (closed shell) Bohr atoms densities (writing "Bohr" for "SqC") are given by

$$\rho_N^{\text{Bohr}}(\mathbf{r}) = 2 \sum_{n=1}^{k_N} \sum_{\ell=0}^{n-1} \sum_{m_\ell=-\ell}^{\ell} |\psi_{n\ell m_\ell}(\mathbf{r})|^2, \quad (28)$$

with the hydrogenic orbitals $\psi_{n\ell m_\ell}(\mathbf{r}) = R_{n\ell}(r) Y_{\ell m_\ell}(\theta, \phi)$ and $k_2 = 1, k_{10} = 2, k_{28} = 3, \dots$

Atomic ions with N **non-interacting** electrons (NIE) and nuclear charge Z obviously have in their ground state exactly the electron density

$$\rho_{Z,N}^{\text{IonNIE}}(\mathbf{r}) = Z^3 \rho_N^{\text{Bohr}}(Z\mathbf{r}) \quad (\text{NIE}). \quad (29)$$

The exact density $\rho_{Z,N}^{\text{Ion}}(\mathbf{r})$ of a **true** atomic ion with $Z \gg N$ asymptotically satisfies

$$\rho_{Z,N}^{\text{Ion}}(\mathbf{r}) \rightarrow \rho_{Z,N}^{\text{IonNIE}}(\mathbf{r}) \quad (Z \gg N). \quad (30)$$

The Bohr atom densities satisfy asymptotic particle-number scaling with $p = -2/3$,

$$\rho_N^{\text{Bohr}}(\mathbf{r}) \approx \bar{\rho}_{N,-2/3}^{\text{TFBohr}}(\mathbf{r}) = \frac{1}{N} \bar{\rho}^{\text{TFBohr}}(N^{-2/3}\mathbf{r}), \quad (31)$$

$$\rho_N^{\text{na}}(\mathbf{r}) \approx \bar{\rho}_{N,+1/3}^{\text{TFna}}(\mathbf{r}) = N^2 \bar{\rho}^{\text{TFna}}(N^{1/3}\mathbf{r}), \quad (32)$$

where we repeated Eq. (25) for the neutral atoms in the second line for comparison.

The TF profile $\bar{\rho}^{\text{TFBohr}}(\mathbf{r})$ has a simple closed form that is reported, for example, in Refs. 43,44. As for neutral atoms, $I_0[\bar{\rho}^{\text{TFBohr}}]$ is finite while $I_2[\bar{\rho}^{\text{TFBohr}}]$ diverges. The divergence of I_2 for both neutral and Bohr atoms has been carefully analysed by Argaman et al.¹⁷

IV. EFFECTIVE SECOND-ORDER GRADIENT EXPANSION

Previous work that used the large- Z (or large- N) neutral atoms data to extract the coefficient B_x numerically, fitted the Z -dependence of the exchange energy for large Z .^{15,17} This procedure relies on knowledge of the large- Z behaviour, which, in view of the diverging nature of I_2 , can easily lead to erroneous assumptions.^{6,15-17} Moreover, a separate fit for each sequence needs to be done.

Here we rely on a different procedure:¹⁶ for a given sequence (SqC) of densities $\rho(\mathbf{r}) = \rho_N^{\text{SqC}}(\mathbf{r})$ with increasing particle number N , we compute an *effective* gradient expansion coefficient

$$\tilde{B}_i^{\text{SqC}}(N) = \frac{W_i[\rho] - W_i^{\text{LDA}}[\rho]}{\int d\mathbf{r} \frac{|\nabla\rho(\mathbf{r})|^2}{\rho(\mathbf{r})^{4/3}}} \Bigg|_{\rho=\rho_N^{\text{SqC}}}. \quad (33)$$

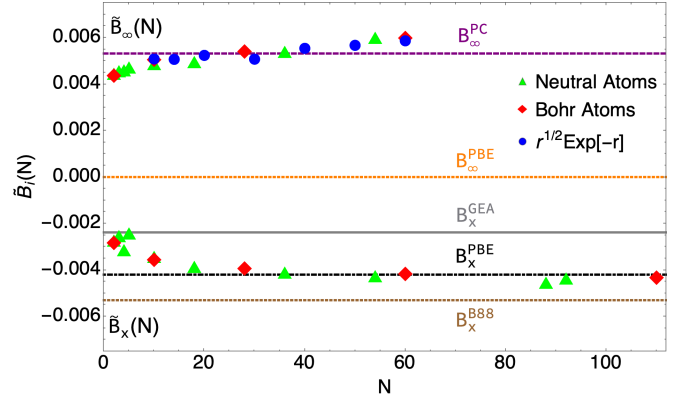


FIG. 1. Numerical values for $\tilde{B}_\infty^{\text{SqC}}(N)$ and $\tilde{B}_x^{\text{SqC}}(N)$ of Eq. (33) for different sequences of densities: **Green: Neutral atoms**, **Red: Bohr atoms**, **Blue: $\rho_N^{\text{SqC}}(\mathbf{r}) = \frac{2N}{15\pi^{3/2}} \sqrt{r} e^{-r}$** . The values for B_i of Table I from the literature are also shown.

As the particle number N increases, the sequence approaches the slowly varying limit (exactly for a scaled profile satisfying Eq. (17), everywhere except in smaller and smaller regions for neutral atoms and Bohr atoms). Therefore, if the GEAs are valid for the functionals $W_i[\rho]$, the numbers $\tilde{B}_i^{\text{SqC}}(N)$ will approach the sought effective coefficients B_i , as explicitly shown in Eq. (19). Whether the B_i will be the same for all sequences (i.e., whether they are profile-independent) is an open question, but this approach allows us to use data from different sequences to address this point more easily than the approach based on fitting the Z -dependence of the energy. It also allows us to combine data obtained by scaled density profiles and data obtained from neutral and Bohr atoms, as the N -dependence of numerator and denominator (whether linear or with logarithmic terms in N) will cancel if the GEA's are valid.

Another way to look at it is the following: if we are interested in using the gradient expansion of Eq. (11) for practical calculations, then we need to use the number $\tilde{B}_i^{\text{SqC}}(N \gg 1)$, hoping that it more or less saturates to a constant value for large N .

A. Densities

The systems we have considered to generate data for $\tilde{B}_i^{\text{SqC}}(N)$ are:

- Closed-shell neutral atoms, treated at the Hartree-Fock level;
- Closed-shell Bohr atoms;
- Only for $B_\infty^{\text{SqC}}(N)$: the particle-number scaled profile $\propto \sqrt{r} e^{-r}$, which was also used in Ref. 26.

The full computational details are reported in the next Sec. VI. However, we should immediately mention that generating accurate data for $W_\infty[\rho]$ with large particle numbers is very challenging. For this reason, data for $B_\infty^{\text{SqC}}(N)$ are limited to $N \leq 60$.

B. Results for the effective gradient expansion

Our results for $B_i^{\text{Sqc}}(N)$ are reported in Fig. 1, together with the various values for B_i from literature of Table I.

The figure shows a surprisingly symmetry: the two extreme limits of correlation for the XC functional seem to have very similar effective gradient expansions in magnitude, but with opposite sign.

The second interesting feature is that the profile-dependence seems rather small, giving some hope for the existence of a universal gradient expansion for finite systems. Regarding exchange, we do not have data with a fixed scaled profile (which would require KS inversion techniques), and thus we do not know whether neutral and Bohr atoms give similar results because of their similar asymptotic diverging behavior of the GEA integral.¹⁷ We should stress that our data are limited to relatively small number of electrons, so it could well be that the asymptotic behavior will eventually be different. However, from a pragmatic point of view, we cover most of the chemically relevant region, and in such region we see that $B_i^{\text{Sqc}}(N)$ becomes reasonably flat. The small increase of $\tilde{B}_\infty^{\text{Sqc}}(N)$ for $N \gtrsim 55$ might also be due to our variational calculations for $W_\infty[\rho]$ being trapped in local minima, as discussed in Sec. VI. For B_∞ , we see that the PC model³⁵ is surprisingly good, especially considering its fully non-empirical derivation, which was based on strictly-correlated electrons in an almost uniform density. The fact that it works so well for finite systems is certainly remarkable. The value obtained from the PBE functional, very close to zero, is clearly incorrect.

For B_x , our Fig. 1 confirms previous studies on gradient expansion and the large- Z neutral atoms,^{5,15,17} extending the conclusions to Bohr atoms, which can now be easily visualised together using our $\tilde{B}_i^{\text{Sqc}}(N)$.

V. IMPLICATIONS FOR THE LIEB-OXFORD BOUND

The LO inequality^{21–23} provides a lower bound for the XC energy in terms of the integral $I_0[\rho]$ of Eq. (9), and has been used as exact constraint in many successful approximations for the XC functional.^{1,7,24} Including the two functionals $E_x[\rho]$ and $W_\infty[\rho]$, the LO bound implies a chain of inequalities,

$$-C \int d^3r \rho(\mathbf{r})^{4/3} \leq W_\infty[\rho] \leq E_{\text{xc}}[\rho] \leq E_x[\rho] \leq 0, \quad (34)$$

where the optimal value of the positive constant C satisfies²³

$$\underbrace{1.44423}_{|A_\infty|} \leq C \leq 1.5765. \quad (35)$$

Dividing Eq. (34) by $-I_0[\rho]$, we obtain

$$0 \leq \frac{-E_x[\rho]}{I_0[\rho]} \leq \frac{-E_{\text{xc}}[\rho]}{I_0[\rho]} \leq \underbrace{\frac{-W_\infty[\rho]}{I_0[\rho]}}_{\Lambda_C[\rho]} \leq C. \quad (36)$$

(Equivalently, the functional $\Lambda[\rho] = \frac{1}{|A_x|} \Lambda_C[\rho]$ has been also used to analyse the LO bound in previous works^{25,26,46}).

The lower bound for C in Eq. (35) corresponds to the highest value of the functional $\Lambda_C[\rho]$ in Eq. (36) ever observed: a floating bcc Wigner crystal with uniform one-electron density.³⁹ The upper bound has been proven in Ref. 23.

Lieb and Oxford²² have also proven that if in Eq. (34) we consider only densities with a fixed number of electrons N , there is an optimal constant $c(N)$ for each N , and that $c(N) \leq c(N+1)$.

The functional $\Lambda_C[\rho]$ has been used in previous works to improve the lower bound for $c(2)$ (which plays a role in XC approximations such as SCAN⁷) and for $c(N \leq 60)$. Since^{26,27}

$$c(N) = \sup_{\rho \rightarrow N} \Lambda_C[\rho], \quad C = \lim_{N \rightarrow \infty} c(N) = \sup_{\rho} \Lambda_C[\rho], \quad (37)$$

improving the lower bounds for $c(N)$ amounts to find densities that give particular high values for $\Lambda_C[\rho]$.

In Refs. 26,27 it was observed that certain density profiles, such as a spherically-symmetric exponential, $\bar{\rho}(\mathbf{r}) \propto e^{-r}$, have very high values of $\Lambda_C[\rho]$ already for small N , while other profiles, such as a sphere of uniform density, yield much lower values. In the next Sec. V A, we use our results of Sec. IV to rationalise this observation.

A. Why are some density profiles more challenging for the LO bound?

In Refs. 26 and 27, values for $\Lambda_C[\bar{\rho}_{N,0}]$ were obtained by using different spherically-symmetric profiles $\bar{\rho}(r)$, with particle-number scaled densities $\bar{\rho}_{N,p}$ defined in Eq. (14). Notice that, due to Eq. (20), $\Lambda_C[\bar{\rho}_{N,p}]$ is independent of p . By inserting Eq. (18) into the definition of $\Lambda_C[\rho]$ of Eq. (36), we see that, for large N ,

$$\Lambda_C[\bar{\rho}_{N,p}] = -A_\infty - B_\infty \frac{I_2[\bar{\rho}]}{I_0[\bar{\rho}]} N^{-2/3} + \dots \quad (38)$$

Since $B_\infty > 0$, the value $-A_\infty > 0$ is approached from below as N grows, indicating that the bcc Wigner crystal value is a local maximum for $\Lambda_C[\rho]$. Moreover, we see that density profiles with small values of the ratio $I_2[\bar{\rho}]/I_0[\bar{\rho}]$ will approach this maximum faster than density profiles for which this ratio is high.

Although the expansion of Eq. (38) is valid for large N , the ratio $I_2[\bar{\rho}]/I_0[\bar{\rho}]$ is an excellent predictor for detecting profiles with high values of Λ_C , already for $N = 2$. This is illustrated in Fig. 2, where the values of $\Lambda_C[\bar{\rho}_{2,0}]$ from Table 1 of Ref. 26, are reported as a function of the corresponding ratio $I_2[\bar{\rho}]/I_0[\bar{\rho}]$. Some of the profiles $\bar{\rho}$ considered in Ref. 26 do not have a finite GEA integral I_2 , and have been excluded from Fig. 2. One such profile is the ‘‘droplet,’’ corresponding to a sphere of uniform density. In this case, the integral I_2 diverges, leading to a different behavior for large N (liquid drop model²⁶), namely

$$\Lambda_C[\bar{\rho}_{N,p}^{\text{Dro}}] = -A_\infty + q_1 N^{-1/3} + q_2 N^{-2/3} + \dots \quad (39)$$

where both q_1 and q_2 are negative.²⁶

If instead of scaled density profiles we use the neutral atoms sequence, we have yet a different large- N dependence, due

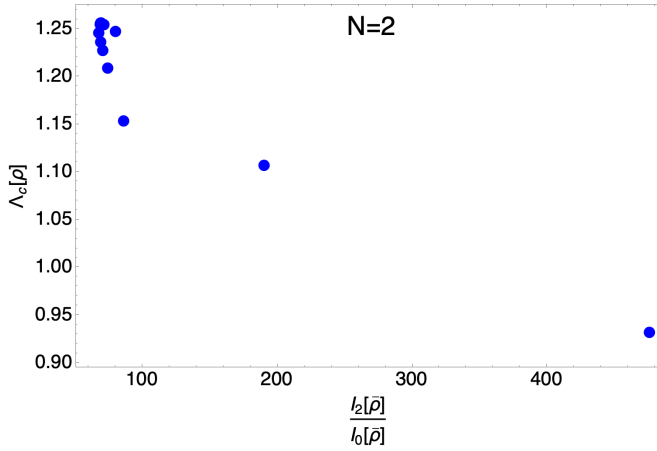


FIG. 2. $\Lambda_C[\bar{\rho}_{2,0}]$ of the different profiles from Table 1 of Ref.26 plotted against the ratio $I_2[\bar{\rho}]/I_0[\bar{\rho}]$ of the GEA and LDA integrals, defined in Eqs. (9)-(10). Densities with an infinite I_2 integral have been excluded.

to the asymptotic divergence of the I_2 integral discussed in Sec. III B 1, namely

$$\Lambda_C[\bar{\rho}_N^{\text{na}}] = -A_\infty - \frac{b_1^{\text{na}}}{a_1^{\text{na}}} N^{-2/3} \log(N) + \dots, \quad (40)$$

where a_1^{na} and b_1^{na} are positive constants appearing in Eqs. (26)-(27). These asymptotic behaviors seem to explain the empirical observation that Λ_C values for uniform droplets approach very slowly the large- N limit,^{25,26} and that neutral atom densities are also not particularly challenging for the LO bound.²⁷

B. The functional $E_{\text{el}}[\rho]$

In this section, we consider the functional $E_{\text{el}}[\rho]$ that appears in the strong-coupling limit of the adiabatic connection (AC) that has the Møller-Plesset (MP) perturbation series as expansion at weak coupling,^{16,28,29}

$$E_{\text{el}}[\rho] = \min_{\{\mathbf{r}_1, \dots, \mathbf{r}_N\}} \left\{ \sum_{i < j=1}^N \frac{1}{|\mathbf{r}_i - \mathbf{r}_j|} - \sum_{i=1}^N \int d^3r \frac{\rho(\mathbf{r})}{|\mathbf{r}_i - \mathbf{r}|} + U[\rho] \right\},$$

$$N = \int \rho(\mathbf{r}) d^3r. \quad (41)$$

The functional $E_{\text{el}}[\rho]$ is the minimum electrostatic energy of a neutral system composed by N identical point charges exposed to a classical continuous charge distribution with charge density $\rho(\mathbf{r})$ of opposite sign, and provides another lower bound^{16,28,29} to the SIL functional, $E_{\text{el}}[\rho] \leq W_\infty[\rho]$. Dividing again by $-I_0[\rho]$, in addition to Eq. (36), we also have

$$\frac{-W_\infty[\rho]}{I_0[\rho]} \leq \frac{-E_{\text{el}}[\rho]}{I_0[\rho]}. \quad (42)$$

The equality is reached for the case of the uniform electron gas (UEG) density,³⁹

$$\frac{-W_\infty[\rho_{\text{UEG}}]}{I_0[\rho_{\text{UEG}}]} = |A_\infty| = \frac{-E_{\text{el}}[\rho_{\text{UEG}}]}{I_0[\rho_{\text{UEG}}]}, \quad (43)$$

where $W_\infty[\rho_{\text{UEG}}]$ is realised by a floating bcc Wigner crystal with uniform density,³⁹ while $E_{\text{el}}[\rho_{\text{UEG}}]$ with any of the equivalent bcc Wigner crystal origins and orientations. The important point is that the two functionals have the same value.³⁹

Values for $E_{\text{el}}[\rho_N^{\text{Sqc}}]$ have been computed for neutral and Bohr atom densities, and for various particle-number scaled profiles in Ref. 16, and are combined, in Fig. 3, with our present data to analyse the relationship with the LO bound. The figure suggests that $-E_{\text{el}}[\rho]/I_0[\rho]$ approaches the UEG value from above.

One could be tempted to think that this is a general feature and that $|A_\infty| \leq -E_{\text{el}}[\rho]/I_0[\rho]$. However, a simple counterexample to this inequality can be found by considering the normalised density profile

$$\bar{\rho}(r) = \frac{(n+2)^{n+3}}{4\pi\Gamma(n+3)} e^{-(n+2)r} r^n, \quad n > 0. \quad (44)$$

As $n \rightarrow \infty$ this density approaches the Dirac measure of the unit sphere. For $N = 1$, the value E_{el} remains finite while I_0 diverges, so their ratio will tend to 0. In such pathological cases then the LO bound becomes very loose, and $E_{\text{el}}[\rho]$ provides a much tighter lower bound to $W_\infty[\rho]$.

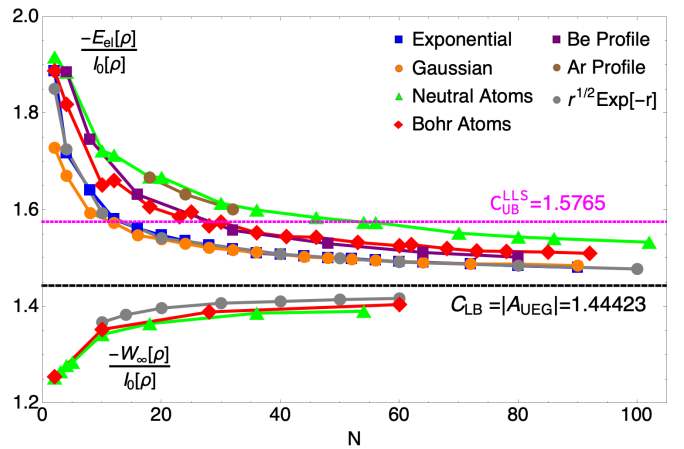


FIG. 3. Numerical values for the functionals $-E_{\text{el}}[\rho]/I_0[\rho]$ and $-W_\infty[\rho]/I_0[\rho]$. Blue: Scaled exponential density. Orange: Scaled gaussian density. Green: Neutral atoms Red: Bohr atoms Purple: Scaled Beryllium profile Brown: Scaled Argon profile Gray: $\rho_N^{\text{Sqc}}(\mathbf{r}) = \frac{2N}{15\pi^{3/2}} \sqrt{r} e^{-r}$. Horizontal black line: $|A_{\text{UEG}}| = |A_\infty|$. Horizontal magenta line: the upper bound $C_{\text{UB}}^{\text{LLS}}$ proven in Ref. 23.

A caveat is that $E_{\text{el}}[\rho]$ has also many local minima. For $W_\infty[\rho]$, this was not a problem, because even if one does not reach the global minimum, the computed value is still variational, providing a rigorous lower bound for C . For $E_{\text{el}}[\rho]$, instead, a local minimum would provide an invalid lower bound to $W_\infty[\rho]$. However, in our experience, the local minima of $E_{\text{el}}[\rho]$ are all very close in energy, so in practice this might not be a severe problem.

VI. COMPUTATIONAL DETAILS

A. Densities

For the neutral atoms, Hartree-Fock calculations were performed using `pyscf` 2.0.1.⁴⁷ An aug-cc-pVQZ⁴⁸ basis set was used, except for Ar (aug-cc-pVDZ⁴⁸), Kr (aug-cc-pVDZ⁴⁸) and Xe (jorge-dzp⁴⁹).

The densities of the Bohr atoms were computed analytically.

B. Exchange functional $E_x[\rho]$

For neutral atoms we used the Hartree-Fock exchange for the calculations described in Sec. VIA above. Although the Hartree-Fock exchange energy is not exactly the same as $E_x[\rho]$ of KS DFT, the two values are very close, and for the qualitative study performed here the small differences should be unimportant. For example for $Z = 10$ our E_x^{HF} is equal to -12.0847 , while the optimized effective potential (OEP) result, E_x^{OEP} , from Ref. 17 is -12.1050 . For $Z = 36$ we have $E_x^{\text{HF}} = -93.805$ and $E_x^{\text{OEP}} = -93.833$.

For the Bohr atoms, the data for $E_x[\rho]$ are taken from Ref. 17.

C. Strong-coupling functional $W_\infty[\rho]$

All the densities considered here have spherical symmetry, and $W_\infty[\rho]$ was computed following the same procedure as in Refs. 18,26,50 and 27. This procedure relies on the radial optimal maps $f_i(r)$ of Ref. 18, which are known to provide either the exact $W_\infty[\rho]$ or a very close variational estimate of it.⁵¹ The calculation also requires a minimization on the relative angles, which becomes very demanding as the number of electrons increases, due to the presence of many local minima. Overall, we can only be sure to provide a variational estimate of $W_\infty[\rho]$, which is obtained as

$$W_\infty[\rho] + U[\rho] = \int_{a_1}^{a_2} 4\pi r^2 \rho(r) V_{ee}(r) dr, \quad (45)$$

where a_1 and a_2 are defined below Eq. (48), and

$$V_{ee}(r) = \sum_{i < j} \frac{1}{|\mathbf{r}_i(r) - \mathbf{r}_j(r)|}. \quad (46)$$

Here, in spherical polar coordinates, $\mathbf{r}_i(r) = (f_i(r), \theta_i(r), \phi_i(r))$ with $i = 1, \dots, N$ is a set of N strictly correlated position vectors, fixed by the distance r of one of the electrons from the origin. The radial maps (or co-motion functions) $f_i(r)$,

$$\underline{R}(r) = (f_1(r), f_2(r), f_3(r), \dots, f_N(r)), \quad (47)$$

with $f_1(r) = r$, are obtained from the density $\rho(r)$ via the cumulant function

$$N_e(r) = \int_0^r 4\pi x^2 \rho(x) dx \quad (48)$$

and its inverse $N_e^{-1}(y)$, as detailed in Ref. 18. For each value of $r \in [a_1, a_2]$, the set of relative angles $\{\theta_i(r), \phi_i(r)\}_{i=1, \dots, N}$

minimises the electron-electron interaction when the radial distances of the electrons from the nucleus are set equal to $\underline{R}(r)$ of Eq. (47). The integration limits in Eq. (45) are $a_k = N_e^{-1}(k)$, with $k = 1$ and 2 (but any pair of adjacent a_k would work, due to cyclic properties of the maps¹⁸).

The electronic densities and co-motion functions were obtained on a 100 000 point Treutler-Ahlrichs grid.⁵² The integration yielding $W_\infty[\rho]$ was performed on an equidistant grid between a_1 and a_2 . The number of grid points for all the Neutral atoms and Bohr atoms were 201, whereas the $\sqrt{r} \exp[-r]$ profile had 203 grid points for $N = 10$, $N = 14$ and $N = 50$, 201 for $N = 40$ and $N = 60$, 103 for $N = 20$ and 99 for $N = 30$. For each $r \in [a_1, a_2]$, we find the minimizing relative angles $\{\theta_i(r), \phi_i(r)\}_{i=1, \dots, N}$ using the Broyden-Fletcher-Goldfarb-Shanno (BFGS) algorithm⁵³⁻⁵⁶ in the `scipy.optimize.minimize` function of `scipy`.⁵⁷

VII. CONCLUSIONS AND PERSPECTIVES

We have analysed gradient expansions of the weak- and strong-coupling functionals $E_x[\rho]$ and $W_\infty[\rho]$ through the lens of particle-number scaling and neutral and Bohr atoms. Our main results are:

- The compact representation in Eq. (33), which allows to analyse an effective gradient expansion for all density sequences at the same time;
- The surprising symmetry in the effective gradient expansions of both functionals, which turn out to be very similar in magnitude but with opposite sign (see Fig. 1);
- A fresh look at the Lieb-Oxford bound for finite N , rationalising why some density profiles give better bounds than others (Sec. VA).

Our findings can be used as constraints in building new XC functionals. For example, the fact that the coefficient of the gradient expansion should become positive at strong-coupling is a constraint ignored in all approximations.

A question that seems to remain open is whether the larger (in magnitude) gradient expansion coefficient for exchange with respect to the one obtained by perturbing an infinite system with uniform density is due to the singular behavior of atomic densities with many electrons close to the nucleus, or whether this coefficient is simply different for finite systems. This question could be answered by computing $E_x[\rho]$ for particle-number scaled densities, Eq. (14), starting from a given profile $\bar{\rho}$ with a finite $I_2[\bar{\rho}]$. This calculation, however, requires a Kohn-Sham inversion for a given density, which is demanding for systems with many particles. For the functional $W_\infty[\rho]$, it seems that a scaled profile and neutral/Bohr atoms give very similar results, although we could only investigate here $N \leq 60$.

ACKNOWLEDGMENTS

This work was funded by the Netherlands Organisation for Scientific Research under Vici grant 724.017.001. We thank

Nathan Argaman, Antonio Cancio and Kieron Burke for the data of the exchange energy of Bohr atoms and for insightful discussions on the gradient expansion, and to Stefan Vuckovic for discussions on the droplet data for the LO bound. We are especially grateful to Mathieu Lewin for suggesting to look at counterexamples of the kind of Eq. (44).

DATA AVAILABILITY

All data will be available on zenodo.

- ¹J. P. Perdew, K. Burke, and M. Ernzerhof, *Phys. Rev. Lett.* **77**, 3865 (1996).
- ²J. P. Perdew, A. Ruzsinszky, J. Tao, V. N. Staroverov, G. E. Scuseria, and G. I. Csonka, *J. Chem. Phys.* **123**, 062201 (2005).
- ³A. J. Cohen, P. Mori-Sánchez, and W. Yang, *Chem. Rev.* **112**, 289 (2012).
- ⁴J. P. Perdew, A. Ruzsinszky, J. Sun, and K. Burke, *The Journal of chemical physics* **140**, 18A533 (2014).
- ⁵J. P. Perdew, L. A. Constantin, E. Sagvolden, and K. Burke, *Phys. Rev. Lett.* **97**, 223002 (2006).
- ⁶J. P. Perdew, A. Ruzsinszky, G. I. Csonka, O. A. Vydrov, G. E. Scuseria, L. A. Constantin, X. Zhou, and K. Burke, *Phys. Rev. Lett.* **100**, 136406 (2008).
- ⁷J. Sun, A. Ruzsinszky, and J. P. Perdew, *Phys. Rev. Lett.* **115**, 036402 (2015).
- ⁸A. M. Teale, T. Helgaker, A. Savin, C. Adamo, B. Aradi, A. V. Arbuznikov, P. W. Ayers, E. J. Baerends, V. Barone, P. Calaminici, E. Cancès, E. A. Carter, P. K. Chattaraj, H. Chermette, I. Ciofini, T. D. Crawford, F. De Proft, J. F. Dobson, C. Draxl, T. Frauenheim, E. Fromager, P. Fuentealba, L. Gagliardi, G. Galli, J. Gao, P. Geerlings, N. Gidopoulos, P. M. W. Gill, P. Gori-Giorgi, A. Görling, T. Gould, S. Grimme, O. Gritsenko, H. J. A. Jensen, E. R. Johnson, R. O. Jones, M. Kaupp, A. M. Köster, L. Kronik, A. I. Krylov, S. Kvaal, A. Laestadius, M. Levy, M. Lewin, S. Liu, P.-F. Loos, N. T. Maitra, F. Neese, J. P. Perdew, K. Pernal, P. Pernot, P. Piecuch, E. Rebolini, L. Reining, P. Romaniello, A. Ruzsinszky, D. R. Salahub, M. Scheffler, P. Schwerdtfeger, V. N. Staroverov, J. Sun, E. Tellgren, D. J. Tozer, S. B. Trickey, C. A. Ullrich, A. Vela, G. Vignale, T. A. Wesolowski, X. Xu, and W. Yang, *Phys. Chem. Chem. Phys.*, (2022).
- ⁹P. R. Antoniewicz and L. Kleinman, *Phys. Rev. B* **31**, 6779 (1985).
- ¹⁰L. Kleinman and S. Lee, *Phys. Rev. B* **37**, 4634 (1988).
- ¹¹P. S. Svendsen and U. Von Barth, *International Journal of Quantum Chemistry* **56**, 351 (1995), <https://onlinelibrary.wiley.com/doi/pdf/10.1002/qua.560560421>.
- ¹²R. van Leeuwen, *Phys. Rev. B* **87**, 155142 (2013).
- ¹³W. Kohn and L. J. Sham, *Phys. Rev.* **140**, A 1133 (1965).
- ¹⁴A. D. Becke, *Phys. Rev. A* **38**, 3098 (1988).
- ¹⁵P. Elliott and K. Burke, *Can. J. Chem.* **87**, 1485 (2009), <https://doi.org/10.1139/V09-095>.
- ¹⁶T. J. Daas, D. P. Kooi, A. J. A. F. Grooteman, M. Seidl, and P. Gori-Giorgi, *Journal of Chemical Theory and Computation* **18**, 1584 (2022), pMID: 35179386, <https://doi.org/10.1021/acs.jctc.1c01206>.
- ¹⁷N. Argaman, J. Redd, A. C. Cancio, and K. Burke, *Phys. Rev. Lett.* **129**, 153001 (2022).
- ¹⁸M. Seidl, P. Gori-Giorgi, and A. Savin, *Phys. Rev. A* **75**, 042511/12 (2007).
- ¹⁹P. Gori-Giorgi, G. Vignale, and M. Seidl, *J. Chem. Theory Comput.* **5**, 743 (2009).
- ²⁰S. Vuckovic, A. Gerolin, T. J. Daas, H. Bahmann, G. Friesecke, and P. Gori-Giorgi, *WIREs Computational Molecular Science* **n/a**, e1634, <https://wires.onlinelibrary.wiley.com/doi/pdf/10.1002/wcms.1634>.
- ²¹E. H. Lieb, *Phys. Lett. A* **70A**, 444 (1979).
- ²²E. H. Lieb and S. Oxford, *Int. J. Quantum. Chem.* **19**, 427 (1981).
- ²³M. Lewin, E. H. Lieb, and R. Seiringer, *Letters in Mathematical Physics* **112** (2022), [10.1007/s11005-022-01584-5](https://doi.org/10.1007/s11005-022-01584-5).
- ²⁴J. P. Perdew and J. Sun, “The lieb-oxford lower bounds on the coulomb energy, their importance to electron density functional theory, and a conjectured tight bound on exchange,” (2022).
- ²⁵E. Räsänen, M. Seidl, and P. Gori-Giorgi, *Phys. Rev. B* **83**, 195111 (2011).
- ²⁶M. Seidl, S. Vuckovic, and P. Gori-Giorgi, *Mol. Phys.* **114**, 1076 (2016).
- ²⁷M. Seidl, T. Benyahia, D. P. Kooi, and P. Gori-Giorgi, “The lieb-oxford bound and the optimal transport limit of dft,” (2022).
- ²⁸M. Seidl, S. Giarrusso, S. Vuckovic, E. Fabiano, and P. Gori-Giorgi, *J. Chem. Phys.* **149**, 241101 (2018).
- ²⁹T. J. Daas, J. Grossi, S. Vuckovic, Z. H. Musslimani, D. P. Kooi, M. Seidl, K. J. H. Giesbertz, and P. Gori-Giorgi, *The Journal of Chemical Physics* **153**, 214112 (2020), <https://doi.org/10.1063/5.0029084>.
- ³⁰M. Levy, *Proc. Natl. Acad. Sci.* **76**, 6062 (1979).
- ³¹E. H. Lieb, *Int. J. Quantum. Chem.* **24**, 243 (1983).
- ³²M. Levy and J. P. Perdew, *Phys. Rev. A* **32**, 2010 (1985).
- ³³M. Levy and J. P. Perdew, *Phys. Rev. B* **48**, 11638 (1993).
- ³⁴G. L. Oliver and J. P. Perdew, *Phys. Rev. A* **20**, 397 (1979).
- ³⁵M. Seidl, J. P. Perdew, and S. Kurth, *Phys. Rev. A* **62**, 012502 (2000).
- ³⁶A. D. Kaplan, M. Levy, and J. P. Perdew, (2022), [10.48550/ARXIV.2207.03855](https://arxiv.org/abs/10.48550/ARXIV.2207.03855).
- ³⁷J. Grossi, D. P. Kooi, K. J. H. Giesbertz, M. Seidl, A. J. Cohen, P. Mori-Sánchez, and P. Gori-Giorgi, *J. Chem. Theory Comput.* **13**, 6089 (2017).
- ³⁸M. Lewin, E. H. Lieb, and R. Seiringer, *Pure and Applied Analysis* **2**, 35 (2020).
- ³⁹M. Lewin, E. H. Lieb, and R. Seiringer, *Phys. Rev. B* **100**, 035127 (2019).
- ⁴⁰E. Fabiano and L. A. Constantin, *Phys. Rev. A* **87**, 012511 (2013).
- ⁴¹E. H. Lieb, *Rev. Mod. Phys.* **53**, 603 (1981).
- ⁴²O. J. Heilmann and E. H. Lieb, *Phys. Rev. A* **52**, 3628 (1995).
- ⁴³A. D. Kaplan, B. Santra, P. Bhattarai, K. Wagle, S. T. u. R. Chowdhury, P. Bhetwal, J. Yu, H. Tang, K. Burke, M. Levy, and J. P. Perdew, *J. Chem. Phys.* **153**, 074114 (2020), <https://doi.org/10.1063/5.0017805>.
- ⁴⁴P. Okun and K. Burke, arXiv preprint arXiv:2105.04384 (2021).
- ⁴⁵D. Lee, L. A. Constantin, J. P. Perdew, and K. Burke, *J. Chem. Phys.* **130**, 034107 (2009), <https://doi.org/10.1063/1.3059783>.
- ⁴⁶E. Räsänen, S. Pittalis, K. Capelle, and C. R. Proetto, *Phys. Rev. Lett.* **102**, 206406 (2009).
- ⁴⁷Q. Sun, T. C. Berkelbach, N. S. Blunt, G. H. Booth, S. Guo, Z. Li, J. Liu, J. D. McClain, E. R. Sayfutyarova, and S. Sharma, *Wiley Interdiscip. Rev.: Comput. Mol. Sci.* **8**, e1340 (2018).
- ⁴⁸R. A. Kendall, T. H. Dunning, and R. J. Harrison, *The Journal of Chemical Physics* **96**, 6796 (1992).
- ⁴⁹F. E. Jorge, A. C. Neto, G. G. Camiletti, and S. F. Machado, *The Journal of Chemical Physics* **130**, 064108 (2009).
- ⁵⁰S. Vuckovic, M. Levy, and P. Gori-Giorgi, *J. Chem. Phys.* **147**, 214107 (2017).
- ⁵¹M. Seidl, S. Di Marino, A. Gerolin, L. Nenna, K. J. Giesbertz, and P. Gori-Giorgi, arXiv preprint arXiv:1702.05022 (2017).
- ⁵²O. Treutler and R. Ahlrichs, *The Journal of Chemical Physics* **102**, 346 (1995).
- ⁵³C. G. Broyden, *IMA J. Appl. Math.* **6**, 76 (1970), <https://academic.oup.com/imamat/article-pdf/6/1/76/2233756/6-1-76.pdf>.
- ⁵⁴R. Fletcher, *Comput. J.* **13**, 317 (1970), <https://academic.oup.com/comjnl/article-pdf/13/3/317/988678/130317.pdf>.
- ⁵⁵D. Goldfarb, *Math. Comput.* **24**, 23 (1970).
- ⁵⁶D. F. Shanno, *Math. Comput.* **24**, 647 (1970).
- ⁵⁷P. Virtanen, R. Gommers, T. E. Oliphant, M. Haberland, T. Reddy, D. Cournapeau, E. Burovski, P. Peterson, W. Weckesser, J. Bright, S. J. van der Walt, M. Brett, J. Wilson, K. J. Millman, N. Mayorov, A. R. J. Nelson, E. Jones, R. Kern, E. Larson, C. J. Carey, Í. Polat, Y. Feng, E. W. Moore, J. VanderPlas, D. Laxalde, J. Perktold, R. Cimrman, I. Henriksen, E. A. Quintero, C. R. Harris, A. M. Archibald, A. H. Ribeiro, F. Pedregosa, P. van Mulbregt, and SciPy 1.0 Contributors, *Nat. Methods* **17**, 261 (2020).